

# Star-Shaped ROMP Polymers Coated with Oligothiophenes That Exhibit Unique Emission

Zelin Sun, Ken Kobori, Kotohiro Nomura,\* and Motoko S. Asano\*

Cite This: *ACS Omega* 2022, 7, 13270–13279

Read Online

ACCESS |



Metrics &amp; More

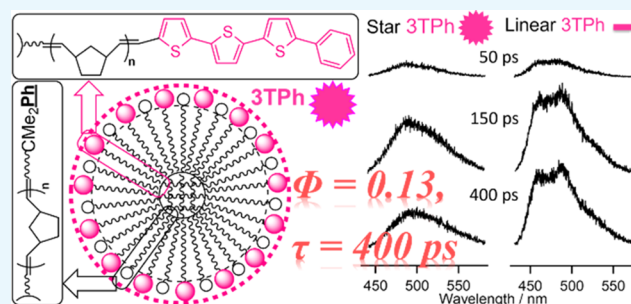


Article Recommendations



Supporting Information

**ABSTRACT:** A series of oligo(thiophene)-modified “soluble” star-shaped ring-opening metathesis polymerization (ROMP) polymers were prepared by sequential living ROMP of norbornene and a cross-linking agent using a molybdenum-alkylidene catalyst, followed by Wittig-type coupling for termination with oligo-(thiophene) carboxaldehydes. The resultant star-shaped ROMP polymers displayed unique emission properties affected by the core size and arm repeat units as well as the kind of oligothiophene coated. The effects of the thiophene groups on photophysical properties of star-shaped/linear polymers were studied *via* time-resolved fluorescence spectroscopy. Fluorescence lifetimes were determined in THF as 400, 640, 730, and 820 ps for **Star 3TPh**, **Linear 3TPh**, **Star 4T**, and **Linear 4T**, respectively. A significant enhancement of the nonradiative rate constants  $k_{nr}$  in the star-shaped polymers results in relatively lower fluorescence quantum yields and shorter fluorescence lifetimes compared to the corresponding linear polymers.



## 1. INTRODUCTION

The study of star-shaped polymers, as one of the simplest nonlinear polymeric materials consisting of linear arms connected at a central branched core, has been an attractive subject, especially in the field of polymer chemistry and materials science.<sup>1–7</sup> The living polymerization technique (absence of undesirable side reactions such as chain transfer and termination, coupling and/or disproportionation *etc.*) plays an essential key role in the precise synthesis, including the end-modification, different and/or block arms (miktoarm stars).<sup>1–7</sup> Among them, the one-pot synthesis by adopting living ring-opening metathesis polymerization (ROMP),<sup>8–15</sup> conducted by the sequential addition of monomers and cross-linkers (CLs),<sup>12,16–37</sup> attracts considerable attention. Two major approaches (Scheme 1), such as arm- (brush) first approach using a ruthenium-carbene catalyst (so-called third-generation Grubbs catalyst)<sup>17–28</sup> and core-first (in and out) approach using a molybdenum-alkylidene catalyst,<sup>29–35</sup> have been known. Moreover, the preparation of cross-linked ROMP polymers applied as monolith materials that are insoluble in common organic solvents was also reported.<sup>8,9,38–40</sup> It was demonstrated that the latter approach using Mo(CHCMe<sub>2</sub>Ph)-(N-2,6-*i*-Pr<sub>2</sub>C<sub>6</sub>H<sub>3</sub>)(O<sup>*t*</sup>Bu)<sub>2</sub> (**Mo cat**) enables us an exclusive synthesis of end-functionalized (surface-modified) star-shaped ROMP polymers<sup>29–35</sup> because the propagating chain end, molybdenum-alkylidene species containing polymer chain, is highly reactive toward aldehyde through Wittig-type coupling.<sup>10,12,41–43</sup> The resultant polymers are size-controlled spherical materials having diameters close to the calculated

values in norbornene (NBE) repeat units through a TEM micrograph (exemplified in Figure 1).<sup>29,30,32</sup>

It has been demonstrated that the resultant star-shaped ROMP polymers by using ruthenium-carbene and molybdenum-alkylidene catalysts can be applied to the materials with better-controlled release/actions,<sup>18,20</sup> magnetic resonance imaging agents,<sup>21,25</sup> and/or degradable materials<sup>28</sup> or supported molecular catalysts<sup>32,35</sup> (by Mo catalyst, Figure 1, bottom; Ti cat.) or unique emitting materials.<sup>31</sup> We demonstrated that oligo(thiophene)-modified (coated) “soluble” star-shaped polymers exhibit unexpected blue emission properties (Figure 1 top). The origin of these unique emission properties could be due to an integration of the ROMP polymers through a space interaction of the oligothiophene moiety with the phenyl group in the initiating fragment. Moreover, the blue emission was turned into a white emission upon the addition of 2-[2-[(*E*)-4-(dimethylamino)styryl]-6-methyl-4*H*-pyran-4-ylidene]malononitrile.<sup>31</sup>

Since we recently demonstrated the one-pot synthesis of end-modified star-shaped polymers with more arms by adopting the living ROMP technique using **Mo cat**, as shown in Scheme 2, we have thus prepared a series of

Received: February 4, 2022

Accepted: March 28, 2022

Published: April 5, 2022





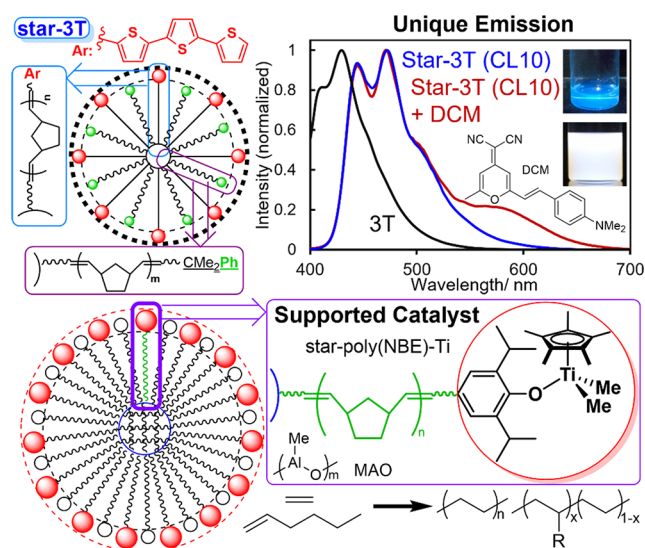


**Figure 1.** End-modified star-shaped polymers containing terthiophene, which show unique emissions [white light emission upon addition of 4-(dicyanomethylene)-2-methyl-6-(4-dimethylaminostyryl)-4Hpyran, left top], phenoxy substituent for supported molecular catalysts (bottom).

As demonstrated in Table 1, the oligo(thiophene)-coated star-shaped ROMP polymers terminated with various aldehydes (2T-CHO, 3T-CHO, MP3T-CHO, 3TPh-CHO, and 4T-CHO, sample names, abbreviations of polymers chosen in this study are also shown in Scheme 2) possessed high molecular weights ( $M_n = 0.98\text{--}2.79 \times 10^5$ , prepared by approaches 1 and 2, Scheme 2) and uniform molecular weight distributions ( $M_w/M_n = 1.27\text{--}1.88$ ). The resultant polymers were highly soluble in ordinary organic solvents, such as toluene, tetrahydrofuran, chloroform, or dichloromethane. It turned out that, as reported previously,<sup>33–35</sup> an increase in CL (10  $\rightarrow$  15 equiv to Mo) resulted in affording the polymers with large  $M_n$  values [e.g.  $M_n = 1.14 \times 10^5$  (run 1) vs  $1.51 \times 10^5$  (run 2);  $1.00 \times 10^5$  (run 7) vs  $1.52 \times 10^5$  (run 8)], suggesting the formation of a star-shaped polymer with increased arm numbers (more branching). The cross-linking density of the polymers could be modified by the addition of NBE (with CL) in the core-formation step [2nd reaction, so-called approach 2, Scheme 2,  $M_n = 1.51 \times 10^5$  (run 2) vs  $1.59 \times 10^5$  (run 3)]. As reported previously, the increase in the NBE amount (NBE/Mo molar ratio) in the third step (from 25 to 50 equiv) led to a notable increase in the  $M_n$  value [e.g.  $M_n = 1.51 \times 10^5$  (run 2) vs  $2.36 \times 10^5$  (run 4)], clearly suggesting the formation of star-shaped ROMP polymers. The resultant star-shaped polymers with different end-groups (runs 2, 6, 8, 10, 14) possessed similar  $M_n$  values ( $1.36\text{--}1.55 \times 10^5$ ) with unimodal molecular weight distributions ( $M_w/M_n = 1.29\text{--}1.54$ ), which are also close to those of the reported star ROMP polymers terminated with 4-pyridinecarboxaldehyde.<sup>32–34</sup>

**2.2. UV–Vis and Fluorescence Spectra of Oligo(thiophene)-Coated Star-Shaped ROMP Polymers.** Figure 2 shows UV–vis ( $1.0 \times 10^{-5}$  M in THF at 25 °C) and fluorescence spectra ( $1.0 \times 10^{-6}$  M in THF at 25 °C) of the oligo(thiophene)-coated star-shaped ROMP polymers, expressed as Star 2T ( $M_n = 155\,000$ ,  $M_w/M_n = 1.33$ , run 6 in Table 1), Star 3T ( $M_n = 152\,000$ ,  $M_w/M_n = 1.29$ , run 8), Star MP3T ( $M_n = 150\,000$ ,  $M_w/M_n = 1.36$ , run 10), Star 3TPh ( $M_n = 151\,000$ ,  $M_w/M_n = 1.54$ , run 2), and Star 4T ( $M_n = 136\,000$ ,

$M_w/M_n = 1.41$ , run 14). Additional UV–vis and fluorescence spectra are shown in the Supporting Information.

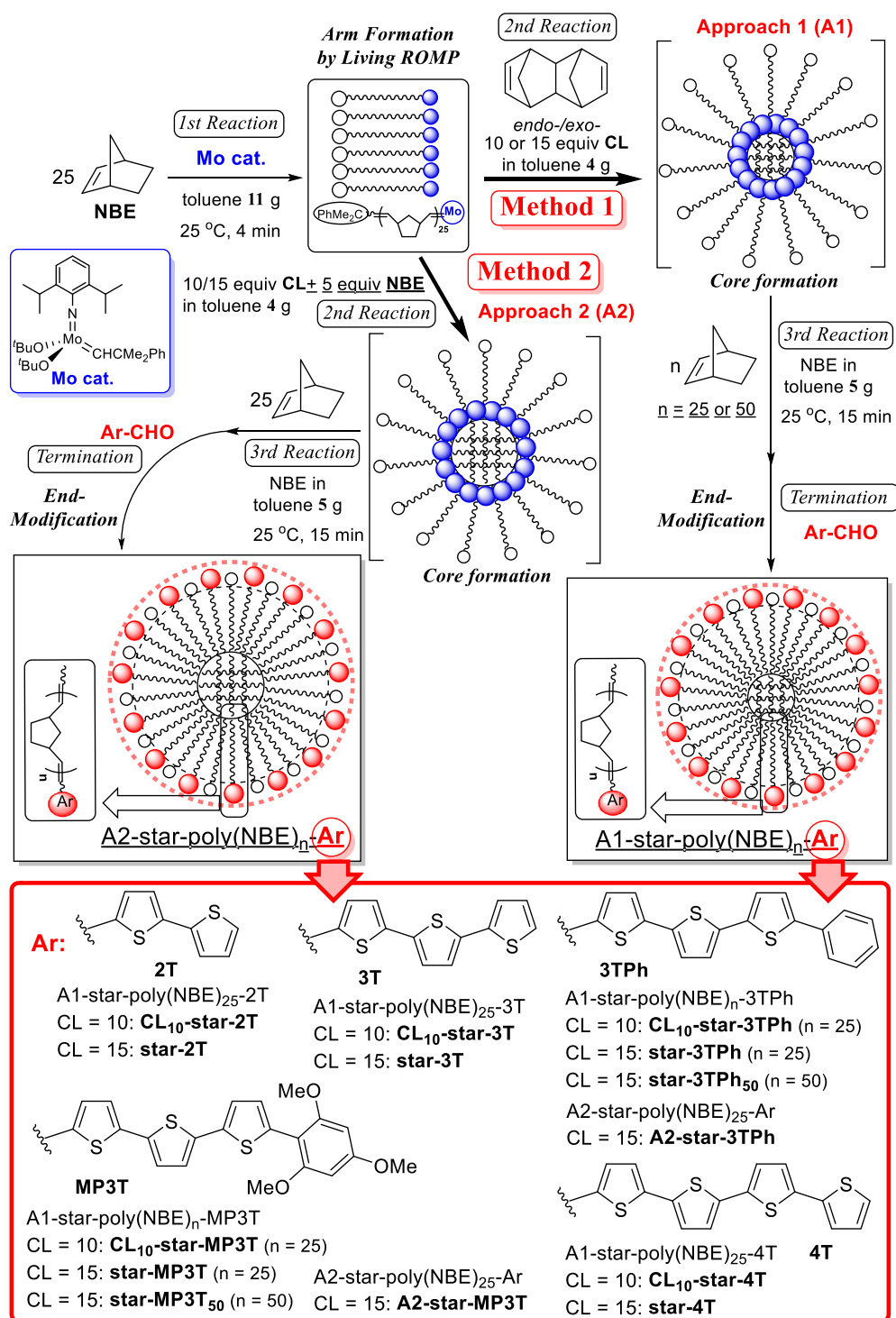
It was revealed that, as shown in Figure 2a, the absorption bands in Star 3T ( $\lambda_{\text{max}} = 388$  nm) and Star 4T (409 nm) were shifted to a longer wavelength relative to those in 3T (354 nm) and 4T (391 nm, Figure S5, Supporting Information),<sup>31</sup> respectively. As reported previously,<sup>31</sup> the observed redshift in these star-shaped polymers could be explained as due to the presence of an interaction of oligo(thiophene) with the phenyl group in the initiation fragment.<sup>31</sup> Similar redshifted absorption bands ( $\lambda_{\text{max}}$  values) were observed in Star MP3T (419 nm), Star 3TPh (412 nm), and Star 4T (409 nm), suggesting an extension of the conjugation units through the interaction. It should be noted that the  $\lambda_{\text{max}}$  value in the absorption in Star 3T (388 nm) is redshifted from its Linear 3T ( $\lambda_{\text{max}} = 377$  nm, Figure S2, Supporting Information), and similar redshifts were observed in the case of Star 2T, Star 3TPh, and Star MP3T (Figures S1, S3, and S4, Supporting Information). In contrast, such a trend was not significant between Star 4T and Linear 4T (Figure S2, Supporting Information) although the reason is not clear at this moment. The observed slight redshift in the  $\lambda_{\text{max}}$  value of Star MP3T compared to that of Star 3TPh (Figure 2a) would be probably attributed to the electron-donating methoxy group that can reduce the HOMO energy level and facilitate the  $p\text{--}\pi$  conjugated effect, thereby reducing the energy of the electronic transition. However, a negligible difference in their emission intensities in higher vibronic bands was observed in their fluorescence spectra (Figure 2b).

It was revealed that  $\lambda_{\text{max}}$  values in the fluorescence spectra (Figure 2b) of Star 4T (479 and 507 nm), Star MP3T (480 and 511 nm), and Star 3TPh (475 and 505 nm) show a longer wavelength relative to those of Star 2T (393 and 413 nm, Figure S6, Supporting Information) and Star 3T (443 and 472 nm). The observed redshifts correspond to the redshifts in their absorption spectra.

Figure 3 (left column) shows fluorescence spectra (in THF at 25 °C with excitation at 410 nm) of the star ROMP polymers containing the same end group (3TPh) prepared with a different NBE length (Star-3TPh<sub>50</sub>, run 4, Table 1), amount of CL (CL<sub>10</sub>-Star-3TPh, run 1), approach in the core formation (addition of NBE in the core formation, Scheme 1, expressed as A2-Star-3TPh, run 3). These spectra were measured in THF with different concentrations ( $1.0 \times 10^{-5}$ ,  $1.0 \times 10^{-6}$ , and  $1.0 \times 10^{-7}$  M on the basis of 3TPh fragment estimated on the basis of molar ratio), as demonstrated previously;<sup>31</sup> the intramolecular interaction (within the star, thiophene, and phenyl group in the initiating fragment) should be more significant than the intermolecular interaction (between the stars) under low concentration conditions. These samples were chosen to study the effects of the cross-linking efficiency (amount of CL, core size) and arm number/length on the emission properties.

The fluorescence intensity in a series of star-shaped polymers containing 3TPh end group (under high concentration conditions,  $1.0 \times 10^{-5}$  M) increased in the order: Star-3TPh, CL<sub>10</sub>-Star-3TPh < A2-Star-3TPh < Star-3TPh<sub>50</sub>. In contrast, the intensity under low concentration conditions ( $1.0 \times 10^{-6}$  M) increased in the order: CL<sub>10</sub>-Star-3TPh  $\ll$  Star-3TPh, A2-Star-3TPh, Star-3TPh<sub>50</sub>. As demonstrated previously,<sup>31</sup> these emissions could be explained as due to the degree of intramolecular and intermolecular interactions between the thiophene group and phenyl group in the

Scheme 2. Synthesis of Oligo(thiophene)-Modified Star-Shaped Polymers by Living ROMP, and Abbreviations of Polymer Samples Employed in This Study



initiation fragment. It was revealed that, in both cases ( $1.0 \times 10^{-5}$ ,  $1.0 \times 10^{-6}$  M), **A2-Star-3TPh** showed higher fluorescence intensities than those in **Star-3TPh**. Moreover, **Star-3TPh** showed higher intensities than those in **CL<sub>10</sub>-Star-3TPh** under low concentration conditions ( $1.0 \times 10^{-6}$  M), whereas a significant difference was not observed under rather high concentration conditions ( $1.0 \times 10^{-5}$  M). These clearly suggest that an increase in these interactions (increase in the intensity) could be explained as due to an increase in arm

numbers, which should facilitate the intramolecular interaction (within the star). Moreover, **Star-3TPh<sub>50</sub>** showed higher fluorescence intensity under low concentration conditions (Figure 3 left), but the degree became close to **A2-Star-3TPh** (and **Star-3TPh**, Figure 3 left). Since the NBE arm containing **3TPh** in **Star-3TPh<sub>50</sub>** should be longer than that containing the phenyl group of the initiating fragment, previously confirmed by both TEM and AFM,<sup>29,30,32</sup> as also explained in our previous report (arm length of two fragments, phenyl

Table 1. Synthesis of Star-Shaped Polymers by Living ROMP (Two Approaches, Scheme 2)<sup>a</sup>

run	2nd			3rd		terminator Ar	$M_n^c \times 10^{-4}$	$M_w/M_n^c$	yield <sup>e</sup> /%	sample name for spectra
	CL <sup>b</sup>	NBE <sup>b</sup>	time/min	NBE <sup>b</sup>	time/min					
1	10	0	50	25	15	3T-Ph	11.4	1.27	85	CL <sub>10</sub> -Star-3TPh
2	15	0	50	25	15	3T-Ph	15.1	1.54	91	Star 3TPh
3	15	5	50	25	15	3T-Ph	15.9	1.58	85	A2-Star-3TPh
4	15	0	50	50	15	3T-Ph	23.6	1.49 <sup>d</sup>	80	Star 3TPh <sub>50</sub>
5	10	0	50	25	15	2T	11.5	1.15	90	CL <sub>10</sub> -Star-2T
6	15	0	50	25	15	2T	15.5	1.33	88	Star 2T
7	10	0	50	25	15	3T	10.0	1.24	84	CL <sub>10</sub> -Star-3T
8	15	0	50	25	15	3T	15.2	1.29	81	Star 3T
9	10	0	50	25	15	MP3T	11.2	1.18	80	CL <sub>10</sub> -Star-MP3T
10	15	0	50	25	15	MP3T	15.0	1.36	83	Star MP3T
11	15	5	50	25	15	MP3T	15.8	1.88	81	A2-Star-MP3T
12	15	0	50	50	15	MP3T	27.9	1.75 <sup>d</sup>	73	Star MP3T <sub>50</sub>
13	10	0	50	25	15	4T	9.8	1.25	90	CL <sub>10</sub> -Star-4T
14	15	0	50	25	15	4T	13.6	1.41	90	Star 4T

<sup>a</sup>Conditions: toluene (total 20.0 g) at 25 °C, Mo cat  $2.00 \times 10^{-5}$  mol (detailed procedure, see Scheme 2). <sup>b</sup>Molar ratio of NBE/Mo or CL/Mo. <sup>c</sup>GPC data in THF vs polystyrene stds. <sup>d</sup>Bimodal molecular weight distribution. <sup>e</sup>Isolated yield (%) as *n*-hexane insoluble fraction.

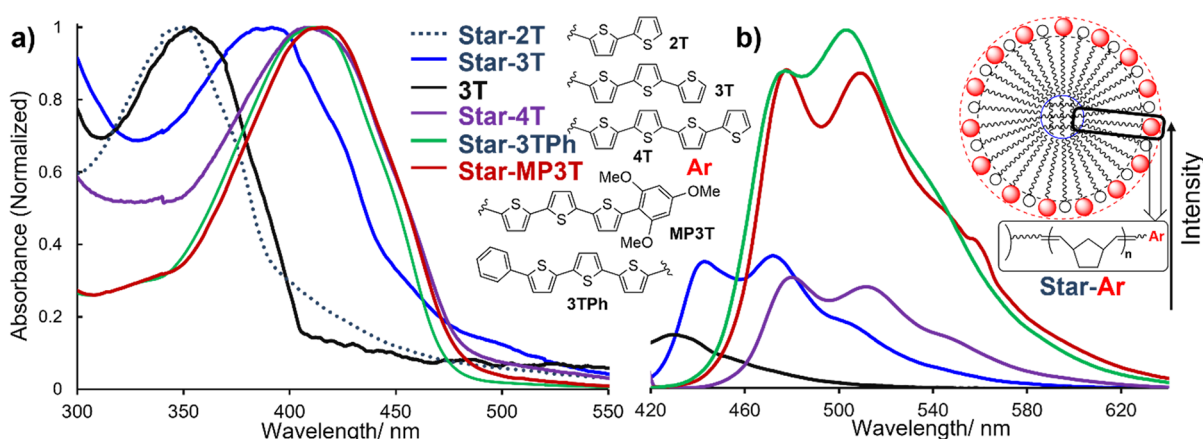


Figure 2. (a) UV-vis spectra [concentration  $1.0 \times 10^{-5}$  M in THF based on oligo(thiophene) units as estimated by the molar ratio at 25 °C] of different types of star-shaped polymers (Star 2T, Star 3T, Star MP3T, Star 3TPh, and Star 4T). (b) Fluorescence spectra of Star 3T, Star MP3T, Star 3TPh, and Star 4T. [Concentration  $1.0 \times 10^{-6}$  M in THF based on oligo(thiophene) units as estimated by the molar ratio at 25 °C, excitation at 390–415 nm ( $\lambda_{\max}$  in the absorption)].

group, and terthiophene, should be close to facilitate the intramolecular interaction),<sup>31</sup> the observed difference could be explained as due to decrease in the intermolecular interaction in Star-3TPh<sub>50</sub>. Taking into account these results, it is clear that both intermolecular and intramolecular interactions can be considered for the observed unique emission, and the fluorescence intensity through the intramolecular interaction should be affected by arm numbers (degree of cross-linking, core size) and the arm length between terthiophene and the phenyl group.

The concentration dependence of the emission spectra was also observed in Star MP3T (Figure 3 right) and Star 3T (Figure S7, Supporting Information); A2-Star-MP3T showed a higher fluorescence intensity than the others, whereas CL<sub>10</sub>-Star-3T and then Star-3T<sub>50</sub> exhibited better intensities. The above fact thus displays the precise placement of both the initiating fragments and the end-functional groups and demonstrates a prerequisite for exhibiting the unique emission, as well as proves the importance of our precise synthesis of star polymers.

### 2.3. Studies on the Optical Properties of Star/Linear 3TPh and Star/Linear 4T. 2.3.1. Steady-State Absorption

and Fluorescence Spectra of Star/Linear 3TPh and Star/Linear 4T. Poly(NBE) is a transparent material (low optical absorbance) that possesses a rather linear structure with semirigidity of its backbone (containing a cyclic structure in the main chain);<sup>43,46,47</sup> the star-, ball-shaped structure with controlled diameters (close to the NBE repeat units) could be thus observed in the TEM micrographs.<sup>29,32,43</sup> In this section, we focus our discussion on comparison between “star” and “linear” polymers by using Star-3TPh ( $M_n = 151\,000$ ,  $M_w/M_n = 1.54$ , run 2), Linear 3TPh ( $M_n = 7000$ ,  $M_w/M_n = 1.10$ , Table S2, run S3), Star 4T ( $M_n = 136\,000$ ,  $M_w/M_n = 1.41$ , run 14), and Linear 4T ( $M_n = 7000$ ,  $M_w/M_n = 1.03$ , Table S2, run S5). As can be seen in Figure S10, their absorption bands could be ascribed to  $\pi$ - $\pi^*$  transitions within the conjugated end-functional groups (3TPh/4T and phenyl group), and no notable differences between the star-shaped and linear polymers were observed. On the other hand, fluorescence spectra vary among these polymers with respect to their vibronic band structures. To confirm whether the fluorescence is from an identical species or not in each polymer, we examined the fluorescence excitation spectra.

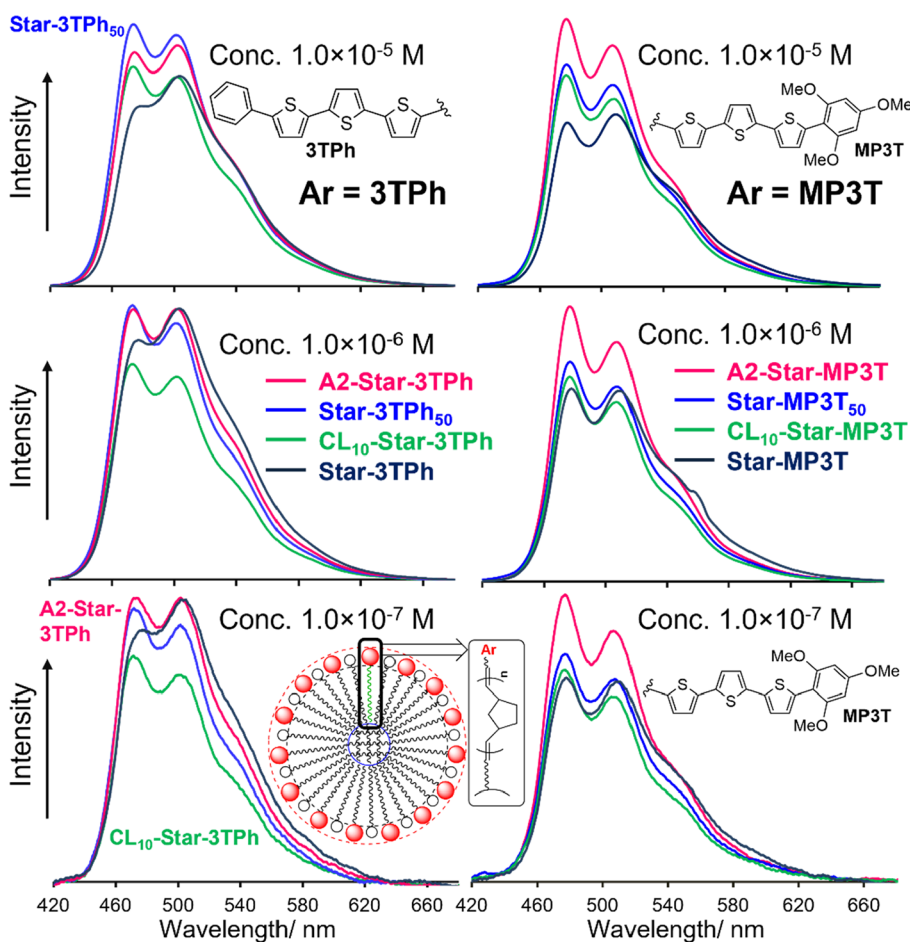


**Figure 3.** Fluorescence spectra of four types of (left) 3TPH- and (right) MP3T-attached star-shaped polymers at different concentrations in THF at 25 °C with excitation at 410 nm. The additional spectra for A2-Star-MP3T and A2-Star-3TPH (with different concentrations) are shown in Figure S9, Supporting Information.

Figure 4 shows the fluorescence excitation spectra of Star/Linear-3TPH and Star/Linear-4T. As can be seen in the

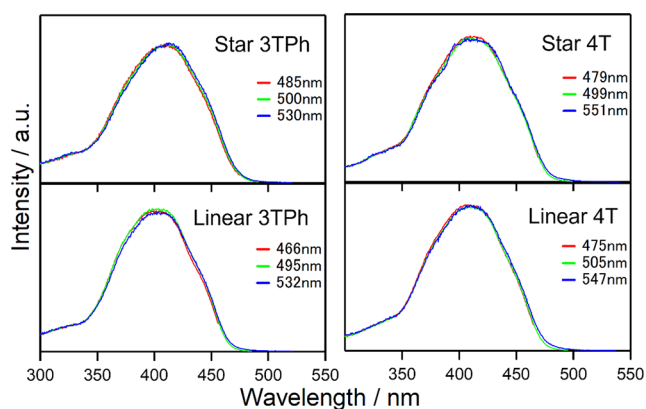


**Figure 4.** Monitored wavelength dependence of excitation spectra of Star/Linear 3TPH and Star/Linear 4T (normalized intensities).

figure, no monitored wavelength dependence was observed in all four polymers, indicating that only one species absorbs light preceding emission in each polymer sample. Moreover, the excitation spectra (Figure 4) are highly matched with the UV-vis absorption spectra, suggesting that there are no other species involved in polymers, that is, the present polymers are

of quite pure quality. Therefore, the fluorescence quantum yields for four polymers (Star-3TPH, Star-4T, Linear-3TPH, and Linear-4T) were further studied for a better understanding of the emission properties of the materials. The wavelengths at the intensity maxima of absorption and emission spectra, along with fluorescence quantum yield in THF, are summarized in Table 2. Fluorescence quantum yields

**Table 2.** Fluorescence Quantum Yields of Star and Linear Polymers (Star 3TPH, Star 4T, Linear 3TPH, and Linear 4T)

samples	absorption $\lambda_{\max}/\text{nm}$	emission $\lambda_{\max}/\text{nm}$	fluorescence quantum yields/ $\phi^a$
Star 3TPH	412	475 500	0.13
Linear 3TPH	407	466 495	0.23
Star 4T	409	479 507	0.20
Linear 4T	409	475 505	0.27

<sup>a</sup>Fluorescence quantum yields with excitation at 426 nm at room temperature.

of Star 3T-Ph, Linear 3T-Ph, Star 4T, and Linear 4T are 0.13, 0.23, 0.20, and 0.27, respectively. A slight redshift of Star 3T-Ph and Star 4T relative to the corresponding linear polymers (Linear 3T-Ph and Linear 4T, respectively) in the maximum emission wavelengths is observed, as shown in Table 2, accompanied by a decrease in their quantum yields. In

comparison to the **Linear 3T-Ph** and **Linear 4T**, fluorescence quantum yields of their star polymers account for 57 and 74%, respectively.

**2.3.2. Dependence of Quantum Yields on the Linear Polymer and Star Polymer.** To clarify the reason for the reduction in quantum yields of star polymers compared with the corresponding linear polymers, time-resolved fluorescence spectra of **Star 3TPh** and **Linear 3TPh** with delay times of 50, 150, and 400 ps from the excitation pulse were investigated in **Figure 5**. The spectral profiles of both **Star 3TPh** and **Linear**

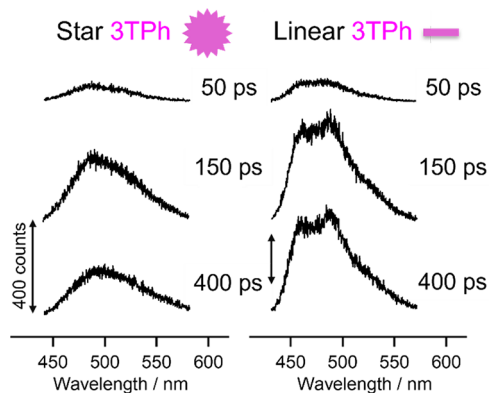


**Figure 5.** Time-resolved fluorescence spectra of star and linear polymers. Delay times from the laser excitation are indicated in the figure. The bar corresponds to 400 counts.

**3TPh** are less time-dependent, indicating no structural change in the excited state. The results of time-resolved fluorescence spectra of **Star 4T** and **Linear 4T** are consistent with those of **Star 3TPh** and **Linear 3TPh**.

**Figure 6** shows time-resolved fluorescence signals of **Star/Linear 3TPh** and **Star/Linear 4T**. All of the decay profiles are

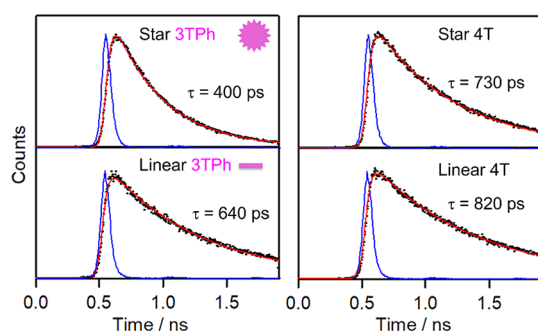


**Figure 6.** Time-resolved fluorescence signals of star and linear polymers excited at 406 nm in THF. Dots express counts of fluorescence signals, whereas the red lines are fittings and blue lines are instrumental responses. The vertical full scale is 6000 counts (**Star 3TPh**), 4600 (**Linear 3TPh**), 2800 (**Star 4T**), and 4300 counts (**Linear 4T**), respectively.

well fitted by a single-exponential decay function, and their fluorescence lifetimes  $\tau$  are listed in **Table 3**. The fluorescence lifetimes of **Star 3TPh**, **Linear 3TPh**, **Star 4T**, and **Linear 4T** are 400, 640, 730, and 820 ps, respectively. Note that a longer fluorescence decay time constant for each linear polymer along with a higher quantum yield was observed than that of the corresponding star polymer.

It is noted that the observed quantum yields and fluorescence lifetimes in these star and linear polymers are

**Table 3. Summary of Emission Lifetime ( $\tau$ ), Fluorescence Quantum Yield ( $\phi$ ), and the Calculated Radiative Rate Constant and Nonradiative Rate Constant ( $k_r$  and  $k_{nr}$ ) of Star and Linear Polymers**

samples	$\tau$ /ps	$\phi^a$	$k_r/s^{-1}$	$k_{nr}/s^{-1}$
<b>Star 3TPh</b>	400	0.13	$3.3 \times 10^8$	$2.2 \times 10^9$
<b>Linear 3TPh</b>	640	0.23	$3.6 \times 10^8$	$1.2 \times 10^9$
<b>Star 4T</b>	730	0.20	$2.7 \times 10^8$	$1.1 \times 10^9$
<b>Linear 4T</b>	820	0.27	$3.2 \times 10^8$	$0.89 \times 10^9$

<sup>a</sup>Fluorescence quantum yields with excitation at 426 nm at room temperature.

much larger than those of terthiophene ( $\phi = 0.07$ ,  $\tau = 160$  ps in benzene) and quaterthiophene ( $\phi = 0.18$ ,  $\tau = 440$  ps in benzene).<sup>48</sup> This is probably due to the effects of expanded  $\pi$ -conjugation over vinyl groups.

In general, quantum yields and lifetimes can be expressed as below<sup>49</sup>

$$\phi = k_r / (k_r + k_{nr}) \quad (1)$$

$$\tau = 1 / (k_r + k_{nr}) \quad (2)$$

where  $k_r$  and  $k_{nr}$  are radiative and nonradiative rate constants, respectively. Based on the observed quantum yields and fluorescence lifetimes by using eqs 1 and 2, values of  $k_r$  and  $k_{nr}$  can be calculated, and the results are presented in **Table 3**.

It should be noted that the  $k_{nr}$  of **Star 3TPh** is enhanced by 1.8 times compared to that of **Linear 3TPh**, and the  $k_{nr}$  of **Star 4T** is 1.2 times higher than that of **Linear 4T**. The significant enhancement of  $k_{nr}$  in star-shaped polymers is attributable to an increase in vibrational modes due to the larger sizes of molecules. The larger number of molecular vibrational modes leads to nonradiative transitions by taking roles as promoting and accepting modes. In addition, the redshifts in star-shaped polymers from the corresponding linear polymers may cause an increase in nonradiative decay rates.

### 3. CONCLUDING REMARKS

The facile one-pot synthesis of highly branched soluble star-shaped polymers containing oligo(thiophene)s has been demonstrated by adopting the living ROMP technique using a molybdenum-alkylidene initiator by simple sequential additions of NBE and a cross-linker coupled with Wittig-type cleavage with an aldehyde in the termination step. The precise placement of both the initiating fragments and the end-functional oligo(thiophene)s is a prerequisite for exhibiting the present unique emission. The unique emission property of the star polymer can be well-maintained at a low concentration *via* controlling the size and arms.

Fluorescence lifetime and fluorescence quantum yield of star/linear polymers with **3TPh** and **4T** as end groups were measured in solution. Radiative and nonradiative constants were estimated. The increased fluorescence lifetime and fluorescence quantum yield of both linear and star polymers functionalized by **4T** was observed compared with those of **3TPh**, mainly caused by a decrease in nonradiative decay. Furthermore, linear polymers possess high values of fluorescence lifetime and quantum yield in comparison with their star polymers terminated with the same functional group because of a decrease in nonradiative decay; however, the values are still comparable to their linear polymers.

Unique emission properties through a space interaction on the star-shaped (non-conjugated) ROMP polymer surface, demonstrated in this work, should provide new possibilities for the design of new functional materials. The results should thus introduce a promising possibility of precision synthesis of star-shaped polymers, placing functionality on the surface.

## 4. EXPERIMENTAL SECTION

**4.1. General Experimental Procedure.** All experiments were conducted in a vacuum atmosphere dry box or by using vacuum/nitrogen lines called Schlenk techniques under a nitrogen ( $N_2$ ) atmosphere. Chemicals of reagent grades were purified by the standard procedures. Toluene was stored over sodium/potassium alloy after pretreatment in a bottle containing molecular sieves (mixture of 3A 1/16, 4A 1/8, and 13X 1/16) from the commercially available one (anhydrous grade, Kanto Chemical Co., Inc.) in the dry box; the polymerization grade toluene was obtained after passing through an alumina flush short column of the supernatant clear solution under  $N_2$ . **Mo cat**<sup>10,12,50</sup> and CL 1,4,4a,5,8,8a-hexahydro-1,4,5,8-*exo-endo*-dimethanonaphtalene (*exo/endo* = 0.15:1.00) were prepared according to the previous reports.<sup>44</sup> **2T-CHO** and **3T-CHO** were used in the dry box as received (Aldrich Chemical Co.) without further purification. **3TPh-CHO**, **MP3T-CHO**, and **4T-CHO** were prepared according to the previous report.<sup>51</sup>

All  $^1H$  and  $^{13}C$  NMR spectra (for confirmation of oligothiophenes<sup>51</sup> and polymers) were measured on a Bruker AV500 spectrometer ( $^1H$ , 500.13 MHz;  $^{13}C$ , 125.77 MHz). All spectra were obtained in the deuterated solvent indicated at 25 °C, and the chemical shifts (in ppm) are referenced to  $SiMe_4$ . Gel-permeation chromatography (GPC) (Shimadzu Co. Ltd.), equipped on a Shimadzu SCL-10A using a RID-10A detector (Shimadzu Co. Ltd.), was used for the measurement of molecular weights and the molecular weight distributions of the resultant star-shaped polymers. GPC measurements were conducted at 40 °C in THF (HPLC grade, Wako Pure Chemical Ind., Inc., degassed prior to use) with the addition of 2,6-di-*tert*-butyl-*p*-cresol (0.03 wt %) at a flow rate of 1.0 mL/min. The molecular weights were estimated on the basis of calibration curves using standard polystyrene samples through GPC columns (ShimPAC GPC-806, 804 and 802, 30 cm  $\times$  8.0 mm  $\phi$ ).

UV-vis spectra (concn  $1.0 \times 10^{-5}$  M in THF at 25 °C) for the resultant polymers were measured by Jasco V-650 UV-vis spectrophotometer, and the fluorescence spectra (ex.  $1.0 \times 10^{-6}$  M in THF at 25 °C) were measured by Hitachi F-7000 fluorescence spectrophotometer or a Horiba FluoroMax 4 spectrophotometer. The resultant polymers were excited at 350–415 nm. The polymer samples were excited at 406 nm by a light pulser Hamamatsu model PLP-10-040 (fwhm 70 ps) for the measurement of time-resolved fluorescence. Emission was dispersed by a Chromex 250IS image spectrograph and detected by a CCD streak scope Hamamatsu model C4334. Both time- and wavelength-resolved data were acquired on a personal computer and then analyzed using lab-made programs. Fluorescence quantum yields of samples were determined relative to that of the PFV oligomer, of which quantum yield was determined as 0.86 in toluene, as described previously.<sup>52</sup>

**4.2. Synthesis of Star/Linear Polymers Containing Different End-Functional Groups, and Synthesis of 3TPh-CHO, MP3T-CHO, and 4T-CHO.** Typical polymer-

ization procedure (run 2, approach 1, Table 1) is as follows.<sup>29–35</sup> Into a toluene solution (10.0 g) containing NBE (25 equiv to Mo, 1.25 mmol, 118 mg),  $Mo(N-2,6-^iPr_2C_6H_3)(CHCMe_2Ph)(O^tBu)_2$  ( $2.00 \times 10^{-5}$  mol) dissolved in toluene (1.0 g) was added in one portion at 25 °C (room temperature). After stirring the reaction mixture for 4 min, a toluene solution (4.0 g) containing 1,4,4a,5,8,8a-hexahydro-1,4,5,8-*exo-endo*-dimethanonaphtalene (CL, 15 equiv to Mo, 0.75 mmol, 119 mg) was added. The solution was stirred for an additional 50 min. Moreover, into the reaction mixture, a toluene solution (5.0 g) containing NBE (25 equiv to Mo, 1.25 mmol, 118 mg) was added in one portion; the solution was further stirred for 15 min. The polymerization was terminated by the addition of **3TPh-CHO** (excess), and the solution was continuously stirred for an additional 1 h for completion. The mixture was then removed *in vacuo* until it was dissolved in the minimum amount of toluene. The solution was poured dropwise into cold *n*-hexane (precooled at  $-30$  °C in the dry box) to afford light yellow precipitates. The polymer was then collected by filtration and dried *in vacuo*. The basic procedure in approach 2 was the same, except that a mixed solution containing CL and NBE (5.0 equiv to Mo in toluene) was added after the initial reaction of 25 equiv of NBE with Mo (second step).  $^1H$  NMR ( $CDCl_3$  at 25 °C) for the star-shaped poly(NBE) main chain:  $\delta$  5.34 and 5.21 (br m, 2H, olefinic), 2.79 and 2.42 (br s, 2H), 1.86 and 1.03 (m, 2H), 1.78,s and 1.35 (m, 4H) ppm. Resonances corresponding to different thiophene end groups 7.00–7.40 (thiophene) were also observed.

Typical linear polymer synthesis procedure: linear ring-opened poly(NBE) containing 3T-Ph as the chain end (**Linear 3TPh**) was prepared under the same conditions except that **3TPh-CHO** was added for termination after the reaction with NBE (only the 1st step in Scheme 2).

## ■ ASSOCIATED CONTENT

### Supporting Information

The Supporting Information is available free of charge at <http://pubs.acs.org/doi/10.1021/acsomega.2c00739>.

Additional data for polymer synthesis, additional UV-vis and fluorescence spectra for polymer samples in THF, temperature-dependent UV-vis and fluorescence spectra in THF, and time-resolved emission spectra of **Star/Linear 4T** (PDF)

## ■ AUTHOR INFORMATION

### Corresponding Authors

Kotohiro Nomura – Department of Chemistry, Graduate School of Science, Tokyo Metropolitan University, Hachioji, Tokyo 192-0397, Japan; [orcid.org/0000-0003-3661-6328](https://orcid.org/0000-0003-3661-6328); Email: [ktnomura@tmu.ac.jp](mailto:ktnomura@tmu.ac.jp); Fax: +81-42-677-2547

Motoko S. Asano – Division of Molecular Science, Graduate School of Science and Technology, Gunma University, Kiryu, Gunma 376-8515, Japan; [orcid.org/0000-0003-2398-8747](https://orcid.org/0000-0003-2398-8747); Email: [motoko@gunma-u.ac.jp](mailto:motoko@gunma-u.ac.jp)

### Authors

Zelin Sun – Department of Chemistry, Graduate School of Science, Tokyo Metropolitan University, Hachioji, Tokyo 192-0397, Japan; Present Address: Department of Applied Biology and Chemical Technology, The Hong Kong

Polytechnic University, Hung Hom, Hong Kong, P. R. China

Ken Kobori – Division of Molecular Science, Graduate School of Science and Technology, Gunma University, Kiryu, Gunma 376-8515, Japan

Complete contact information is available at:

<https://pubs.acs.org/10.1021/acsomega.2c00739>

## Notes

The authors declare no competing financial interest.

## ACKNOWLEDGMENTS

This project was partly supported by Grants-in-Aid for Challenging Exploratory Research (18K18981, 21K18854) and Scientific Research (17K05801, 20K05679) and the Japan Society for the Promotion of Science (JSPS). Sho Hashimoto and Takahiro Hagiwara (Gunma University) are acknowledged for their assistance in measurements of time-resolved and temperature dependence of fluorescence spectra.

## ADDITIONAL NOTE

<sup>a</sup>According to the method employed previously,<sup>29,35</sup> the number of arms containing oligothiophene moieties in the resultant star-shaped ROMP polymers could be speculated on the basis of GPC data for poly(NBE)<sub>25</sub> (linear ROMP polymer prepared with 25 equiv of NBE,  $M_n = 2350$  by GPC in THF vs polystyrene standards) and poly(NBE)<sub>50</sub> ( $M_n = 4710$ ).<sup>34</sup> It was thus speculated that the resultant star-shaped ROMP polymers [runs 2 and 4,  $M_n = 15\ 100, 236\ 000$  (for 3T-Ph); runs 10 and 12,  $M_n = 15\ 000, 279\ 000$  (for MP3T), respectively] possessed ca. 36 (3T-Ph), 55 (MP3T) poly(NBE) arms containing the oligothiophene moiety. However, the exact arm numbers could not be estimated in the present study and the reported studies.<sup>16–36</sup>

## REFERENCES

- (1) Hadjichristidis, N.; Pitsikalis, M.; Pispas, S.; Iatrou, H. Polymers with complex architecture by living anionic polymerization. *Chem. Rev.* **2001**, *101*, 3747–3792.
- (2) Hirao, A.; Hayashi, M.; Loykulant, S.; Sugiyama, K.; Ryu, S.; Haraguchi, N.; Matsuo, A.; Higashihara, T. Precise syntheses of chain-multi-functionalized polymers, star-branched polymers, star-linear block polymers, densely branched polymers, and dendritic branched polymers based on iterative approach using functionalized 1,1-diphenylethylene derivatives. *Prog. Polym. Sci.* **2005**, *30*, 111–182.
- (3) Matyjaszewski, K.; Tsarevsky, N. V. Nanostructured functional materials prepared by atom transfer radical polymerization. *Nat. Chem.* **2009**, *1*, 276–288.
- (4) Khanna, K.; Varshney, S.; Kakkar, A. Miktoarm star polymers: advances in synthesis, self-assembly, and applications. *Polym. Chem.* **2010**, *1*, 1171–1185.
- (5) Matyjaszewski, K.; Tsarevsky, N. V. Macromolecular engineering by atom transfer radical polymerization. *J. Am. Chem. Soc.* **2014**, *136*, 6513–6533.
- (6) Ren, J. M.; McKenzie, T. G.; Fu, Q.; Wong, E. H. H.; Xu, J.; An, Z.; Shanmugam, S.; Davis, T. P.; Boyer, C.; Qiao, G. G. Star polymers. *Chem. Rev.* **2016**, *116*, 6743–6836.
- (7) Liu, Y.; Wang, J.; Zhang, M.; Li, H.; Lin, Z. Polymer-ligated nanocrystals enabled by nonlinear block copolymer nanoreactors: Synthesis, properties, and applications. *ACS Nano* **2020**, *14*, 12491–12521.
- (8) Buchmeiser, M. R. Homogeneous metathesis polymerization by well-defined group VI and group VIII transition-metal alkylidenes: Fundamentals and applications in the preparation of advanced materials. *Chem. Rev.* **2000**, *100*, 1565–1604.

(9) *Handbook of Metathesis*; Grubbs, R. H., Ed.; Wiley-VCH: Weinheim, Germany, 2003; Vol. 3.

(10) Schrock, R. R. Recent advances in high oxidation state Mo and W imido alkylidene chemistry. *Chem. Rev.* **2009**, *109*, 3211–3226.

(11) Hilf, S.; Kilbinger, A. F. M. Functional end groups for polymers prepared using ring-opening metathesis polymerization. *Nat. Chem.* **2009**, *1*, 537–546.

(12) Nomura, K.; Abdellatif, M. M. Precise synthesis of polymers containing functional end groups by living ring-opening metathesis polymerization (ROMP): Efficient tools for synthesis of block/graft copolymers. *Polymer* **2010**, *51*, 1861–1881.

(13) Leitgeb, A.; Wappel, J.; Slugovc, C. The ROMP toolbox upgraded. *Polymer* **2010**, *51*, 2927–2946.

(14) *Handbook of Metathesis*, 2nd ed.; Grubbs, R. H., Khosravi, E., Eds.; Wiley-VCH: Weinheim, Germany, 2015; Vol. 3.

(15) Chen, Y.; Abdellatif, M. M.; Nomura, K. Olefin metathesis polymerization: Some recent developments in the precise polymerizations for synthesis of advanced materials (by ROMP, ADMET). *Tetrahedron* **2018**, *74*, 619–643.

(16) Arm (brush) first approach by addition of cross-linked reagent(s) at the final stage (refs 16–28) Saunders, R. S.; Cohen, R. E.; Wong, S. J.; Schrock, R. R. Synthesis of amphiphilic star block copolymers using ring-opening metathesis polymerization. *Macromolecules* **1992**, *25*, 2055–2057.

(17) Liu, J.; Burts, A. O.; Li, Y.; Zhukhovitskiy, A. V.; Ottaviani, M. F.; Turro, N. J.; Johnson, J. A. “Brush-first” method for the parallel synthesis of photocleavable, nitroxide-labeled poly (ethylene glycol) star polymers. *J. Am. Chem. Soc.* **2012**, *134*, 16337–16344.

(18) Liao, L.; Liu, J.; Dreaden, E. C.; Morton, S. W.; Shopsowitz, K. E.; Hammond, P. T.; Johnson, J. A. A convergent synthetic platform for single-nanoparticle combination cancer therapy: Ratiometric loading and controlled release of cisplatin, doxorubicin, and camptothecin. *J. Am. Chem. Soc.* **2014**, *136*, 5896–5899.

(19) Burts, A. O.; Gao, A. X.; Johnson, J. A. Brush-first synthesis of core-photodegradable miktoarm star polymers via ROMP: Towards photoresponsive self-assemblies. *Macromol. Rapid Commun.* **2014**, *35*, 168–173.

(20) Barnes, J. C.; Bruno, P. M.; Nguyen, H. V.-T.; Liao, L.; Liu, J.; Hemann, M. T.; Johnson, J. A. Using an RNAi signature assay to guide the design of three-drug-conjugated nanoparticles with validated mechanisms, in vivo efficacy, and low toxicity. *J. Am. Chem. Soc.* **2016**, *138*, 12494–12501.

(21) Nguyen, H. V.-T.; Chen, Q.; Paletta, J. T.; Harvey, P.; Jiang, Y.; Zhang, H.; Boska, M. D.; Ottaviani, M. F.; Jasanoff, A.; Rajca, A.; Johnson, J. A. Nitroxide-based macromolecular contrast agents with unprecedented transverse relaxivity and stability for magnetic resonance imaging of tumors. *ACS Cent. Sci.* **2017**, *3*, 800–811.

(22) Shibuya, Y.; Nguyen, H. V.-T.; Johnson, J. A. Mikto-brush-arm star polymers via cross-linking of dissimilar bottlebrushes: Synthesis and solution morphologies. *ACS Macro Lett.* **2017**, *6*, 963–968.

(23) Nguyen, H. V.-T.; Gallagher, N. M.; Vohidov, F.; Jiang, Y.; Kawamoto, K.; Zhang, H.; Park, J. V.; Huang, Z.; Ottaviani, M. F.; Rajca, A.; Johnson, J. A. Scalable synthesis of multivalent macromonomers for ROMP. *ACS Macro Lett.* **2018**, *7*, 472–476.

(24) Rokhlenko, Y.; Kawamoto, K.; Johnson, J. A.; Osuji, C. O. Sub-10 nm self-assembly of mesogen-containing grafted macromonomers and their bottlebrush polymers. *Macromolecules* **2018**, *51*, 3680–3690.

(25) Nguyen, H. V.-T.; Detappe, A.; Gallagher, N. M.; Zhang, H.; Harvey, P.; Yan, C.; Mathieu, C.; Golder, M. R.; Jiang, Y.; Ottaviani, M. F.; Jasanoff, A.; Rajca, A.; Ghobrial, I.; Ghoroghchian, P. P.; Johnson, J. A. Triply loaded nitroxide brush-arm star polymers enable metal-free millimetric tumor detection by magnetic resonance imaging. *ACS Nano* **2018**, *12*, 11343–11354.

(26) Golder, M. R.; Nguyen, H. V.-T.; Oldenhuis, N. J.; Grundler, J.; Park, E. J.; Johnson, J. A. Brush-first and ROMP-out with functional (macro)monomers: method development, structural investigations, and applications of an expanded brush-arm star polymer platform. *Macromolecules* **2018**, *51*, 9861–9870.

- (27) Alvaradejo, G. G.; Nguyen, H. V.-T.; Harvey, P.; Gallagher, N. M.; Le, D.; Ottaviani, M. F.; Jasanoff, A.; Delaittre, G.; Johnson, J. A. Polyoxazoline macromonomers for ROMP: synthesis, functionalization, and application as nitroxide-based organic radical contrast agents. *ACS Macro Lett.* **2019**, *8*, 473–478.
- (28) Shieh, P.; Nguyen, H. V.-T.; Johnson, J. A. Tailored silyl ether monomers enable backbone-degradable polynorbornene-based linear, bottlebrush and star copolymers through ROMP. *Nat. Chem.* **2019**, *11*, 1124–1132.
- (29) In and out (modified core first) approach (refs 29–35): Nomura, K.; Watanabe, Y.; Fujita, S.; Fujiki, M.; Otani, H. Facile controlled synthesis of soluble star shape polymers by ring-opening metathesis polymerization (ROMP). *Macromolecules* **2009**, *42*, 899–901.
- (30) Otani, H.; Fujita, S.; Watanabe, Y.; Fujiki, M.; Nomura, K. A facile, controlled synthesis of soluble star polymers containing a sugar residue by ring-opening metathesis polymerization (ROMP). *Macromol. Symp.* **2010**, *293*, 53–57.
- (31) Takamizu, K.; Nomura, K. Synthesis of oligo(thiophene) coated star shape ROMP polymers: Unique emission properties by the precise integration of functionality. *J. Am. Chem. Soc.* **2012**, *134*, 7892–7895.
- (32) Nomura, K.; Tanaka, K.; Fujita, S. Use of pyridine coated star shape ROMP polymers as the supported ligand for Ru-catalyzed chemoselective hydrogen transfer reduction of ketones. *Organometallics* **2012**, *31*, 5074–5080.
- (33) Sun, Z.; Nomura, K. One-pot synthesis of end-functionalised soluble star-shaped polymers by living ring-opening metathesis polymerisation using molybdenum-alkylidene catalyst. *RSC Adv.* **2018**, *8*, 27703–27708.
- (34) Sun, Z.; Morishita, K.; Nomura, K. Synthesis of soluble star-shaped polymers via in and out approach by ring-opening metathesis polymerization (ROMP) of norbornene: Factors affecting the precise synthesis. *Catalysts* **2018**, *8*, 670.
- (35) Sun, Z.; Unruean, P.; Aoki, H.; Kitiyanan, B.; Nomura, K. Phenoxide-modified half-titanocenes supported on star-shaped ROMP polymers as efficient catalyst precursors for ethylene copolymerization. *Organometallics* **2020**, *39*, 2998–3009.
- (36) Other approaches (refs 36–41) Kalow, J. A.; Swager, T. M. Synthesis of miktoarm branched conjugated copolymers by ROMPing in and out. *ACS Macro Lett.* **2015**, *4*, 1229–1233.
- (37) Levi, A. E.; Fu, L.; Lequieu, J.; Horne, J. D.; Blankenship, J.; Mukherjee, S.; Zhang, T.; Fredrickson, G. H.; Gutekunst, W. R.; Bates, C. M. Efficient synthesis of asymmetric miktoarm star polymers. *Macromolecules* **2020**, *53*, 702–710.
- (38) Lubbad, S.; Buchmeiser, M. R. A new approach to high-capacity functionalized monoliths via post-synthesis grafting. *Macromol. Rapid Commun.* **2003**, *24*, 580–584.
- (39) Mayr, M.; Wang, D.; Kröll, R.; Schuler, N.; Prühs, S.; Fürstner, A.; Buchmeiser, M. R. Monolithic disk-supported metathesis catalysts for use in combinatorial chemistry. *Adv. Synth. Catal.* **2005**, *347*, 484–492.
- (40) Buchmeiser, M. R. Polymer-supported well-defined metathesis catalysts. *Chem. Rev.* **2009**, *109*, 303–321.
- (41) Schrock, R. R. In *Handbook of Metathesis*; Grubbs, R. H., Ed.; Wiley-VCH: Weinheim, 2003; Vol. 1, pp 8–32.
- (42) Nomura, K.; Takahashi, S.; Imanishi, Y. Synthesis of poly(macromonomer)s by repeating ring-opening metathesis polymerization (ROMP) with Mo(CHCMe<sub>2</sub>Ph)(NAr)(OR)<sub>2</sub> initiators. *Macromolecules* **2001**, *34*, 4712–4723.
- (43) Murphy, J. J.; Furusho, H.; Paton, R. M.; Nomura, K. Precise synthesis of poly(macromonomer)s containing sugars by repetitive ROMP and their attachments to poly(ethylene glycol): synthesis, TEM analysis and their properties as amphiphilic block fragments. *Chem.—Eur. J.* **2007**, *13*, 8985–8997.
- (44) Stille, J. K.; Frey, D. A. Tetracyclic dienes. I. The diels-alder adduct of norbornadiene and cyclopentadiene. *J. Am. Chem. Soc.* **1959**, *81*, 4273–4275.
- (45) Asano, M. S.; Kagota, D.; Haque, T.; Koinuma, M.; Inagaki, A.; Nomura, K. Time-resolved fluorescence spectra in the end-functionalized conjugated triblock copolymers consisting of poly(fluorene vinylene) and oligo(phenylene vinylene): Proposal of dynamical distortion in the excited state. *Macromolecules* **2015**, *48*, 6233–6240.
- (46) For example (refs 29 32 43 46, and 47) Gestwicki, J. E.; Cairo, C. W.; Strong, L. E.; Oetjen, K. A.; Kiessling, L. L. Influencing receptor-ligand binding mechanisms with multivalent ligand architecture. *J. Am. Chem. Soc.* **2002**, *124*, 14922–14933.
- (47) Kiessling, L. L.; Gestwicki, J. E.; Strong, L. E. Synthetic multivalent ligands as probes of signal transduction. *Angew. Chem., Int. Ed.* **2006**, *45*, 2348–2368.
- (48) Becker, R. S.; Seixas de Melo, J.; Maçanita, A. L.; Elisei, F. Comprehensive evaluation of the absorption, photophysical, energy transfer, structural, and theoretical properties of  $\alpha$ -oligothiophenes with one to seven rings. *J. Phys. Chem.* **1996**, *100*, 18683–18695.
- (49) Asano, M. S.; Yasuda, Y.; Kagota, D.; Haque, T.; Nomura, K. Effects of terthiophene as the end-groups in triblock copolymers consisting of poly(fluorene vinylene) and oligo(phenylene vinylene): Time-resolved fluorescence and its anisotropy. *J. Photochem. Photobiol., A* **2017**, *349*, 18–24.
- (50) Schrock, R. R.; Murdzek, J. S.; Bazan, G. C.; Robbins, J.; Dimare, M.; O'Regan, M. Synthesis of molybdenum imido alkylidene complexes and some reactions involving acyclic olefins. *J. Am. Chem. Soc.* **1990**, *112*, 3875–3886.
- (51) Kuwabara, S.; Yamamoto, N.; Sharma, P. M. V.; Takamizu, K.; Fujiki, M.; Geerts, Y.; Nomura, K. Precise synthesis of poly(fluorene-2,7-vinylene)s containing oligo(thiophene)s at the chain ends: Unique emission properties by the end functionalization. *Macromolecules* **2011**, *44*, 3705–3711.
- (52) Fushimi, Y.; Koinuma, M.; Yasuda, Y.; Nomura, K.; Asano, M. S. Effects of end-groups on photophysical properties of poly(9,9-di-n-octylfluorene-2,7-vinylene)s linked with metalloporphyrins: Synthesis and time-resolved fluorescence spectroscopy. *Macromolecules* **2017**, *50*, 1803–1814.